communications earth & environment

Article

A Nature Portfolio journal

https://doi.org/10.1038/s43247-025-03064-9

Glacier-specific controls on enhanced trace metal mobility across global mountain and polar meltwaters

Check for updates

Shipika Sundriyal[1], Tanuj Shukla[1] ✉, Shichang Kang[1,2,3], Yulang Zhang[1], Rajesh Singh[4], Uday Bhan[5] & D. P. Dobhal[6]

Glacier retreat, a consequence of climate warming, raises concerns about the release of tracemetals previously locked within ice, yet the global patterns and governing mechanisms of their mobilization remain unclear. Here we present dissolved trace metal data from 14 mountain glaciers and 2 polar ice sheets to quantify how glacier-type governs elemental mobilization. Both glacier classes release meltwaters with concentrations that often exceed global riverine and open-ocean means by one to two orders of magnitude, yet their chemical signatures differ. Mountain-glacier meltwaters are enriched in essential micronutrients such as Zn, Co, Ni, Cd, and Cu relative to ice sheets. These disparities reflect enhanced weathering, lithological diversity, and greater availability of freshly ground particles in alpine systems. These fluxes fertilize nutrient-limited ecosystems yet also elevate metal toxicity. This contrast underscores that differences between glacier type will determine how ice loss reshapes the future balance between micronutrient supply and contaminant release under accelerating glacier and ice-sheet retreat.

Glaciers and their meltwaters represent active geochemical systems that both store and release trace metals (TMs). Atmospheric deposition accumulates in snow and firn, sequestering TMs within the ice column until melt onset, while subglacial abrasion exposes reactive mineral surfaces that enhance dissolution and metal fluxes to runoff[1,2]. Thus, glacier fed streams, often regarded as freshwater resources, transport measurable loads of dissolved metals, raising a fundamental question: how, and to what extent, do cryospheric processes contribute to TM fluxes in natural waters? Although numerous local studies have reported enrichment of elements such as Pb, Zn, and Fe in glacial meltwaters[2], the global role of glaciers in TMs export remains poorly highlighted. The urgency of this question is underscored by the rapid loss of glacier ice worldwide: mountain glaciers (1–100 km^2) are retreating at unprecedented rates, with total global ice loss exceeding 267 ± 19 Gt yr^{-1} [3–5]. In the Himalaya alone, glacier mass loss has nearly doubled over the past four decades, from −0.22 ± 0.13 to −0.43 ± 0.14 m w.e. yr^{-1} [3–5]. This accelerated melt not only threatens water resources but also releases legacy TMs previously sequestered in ice and subglacial sediments, influencing downstream water quality, nutrient supply, and contaminant fluxes[1].

The contrast between small mountain glaciers and vast ice sheets (>50,000 km^2) further highlights this urgency. Ice sheet studies from Greenland and Antarctica demonstrate that meltwater derived Fe, Mn, and Zn exert measurable influence on marine productivity and large scale biogeochemical cycling[4,6–8]. In contrast, mountain glaciers, numbering over 200,000 globally, drain highly heterogeneous lithologies and climatic regimes, producing meltwaters through short-lived, high energy drainage networks that enhance mineral–water interactions and TM fluxes. These turbulent flows enhance rock-water interaction, intensify sulfide and carbonate weathering, and accelerate TMs mobilization[1–8]. Beneath ice sheets, however, longer residence times and distributed drainage networks foster suboxic conditions by favoring sulfide oxidation and Fe(III) reduction[8]. Such contrasting hydrological regimes yield distinct chemical signatures: mountain glaciers act as lithologic amplifiers of TMs release, whereas ice sheets operate as redox reactors regulating solute export under anoxic confinement[1,8]. Yet, no comprehensive comparison has previously evaluated these differences on a global scale. Existing studies have typically focused on single glacier catchments[9] or isolated ice sheet basins[2], leaving the broader cryospheric contribution unresolved.

[1]State Key Laboratory of Cryospheric Science and Frozen Soil Engineering, Northwest Institute of Eco-Environment and Resources, Chinese Academy of Sciences, Lanzhou, China. [2]University of Chinese Academy of Sciences (UCAS), Beijing, China. [3]Institute of Mountain Hazards and Environment, Chinese Academy of Sciences, Chengdu, China. [4] Environmental Hydrology Division, National Institute of Hydrology, Roorkee, India. [5]University of Petroleum and Energy Studies (UPES), Dehradun, India. [6]Wadia Institute of Himalayan Geology, Dehradun, India. ✉e-mail: tanuj.shukla@nieer.ac.cn

To address this gap, we apply two complementary geochemical diagnostics that quantify elemental enrichment and mobility. Enrichment factors (EFs) express the ratio of TM concentrations in glacier meltwater to their upper-continental crust (UCC) abundances, with EF ≫ 1 indicating excess inputs from atmospheric or anthropogenic sources[10]. Mobility indices (MIs), by contrast, normalize TM concentrations first to their crustal abundance and then to a reference element, reflecting each element's relative transport efficiency. Together, EFs and MIs disentangle lithogenic versus atmospheric influences and provide a quantitative measure of weathering intensity across glacier types[2,9,10]. We compiled the cross-cryosphere dataset of dissolved TM concentrations till date from 16 glacier catchments worldwide. This dataset spans the Himalaya, Tibetan plateau, Andes, Rocky Mountain, and European Alps, and it integrates new field data (Dokriani Glacier; Gangotri Glacier) with published results from Greenland and Antarctic ice sheets. The dataset includes <0.45 µm dissolved concentrations for 17 elements (Supplementary Tables S2–S6) and integrates new field data from the Dokriani (DG) and Gangotri Glaciers (GG) with published results from Leverett Glacier (GIS), Mercer Subglacial Lake (AIS), Laohugou Glacier (Tibetan plateau)[11], and representative basins from the Alps[12–14], Andes[15–17], and Rocky Mountain[18,19] (Fig. 1). Our field assessments particularly from the Himalaya and the Tibetan Plateau reveal that elevated dissolved metal concentrations in meltwaters reflect intensified glacial melt, enhanced subglacial weathering, and evolving hydrological flow paths under ongoing climatic change[20–22]. We quantify glacier type contrasts using Spearman correlations, Mann–Whitney *U* tests, Cliff's δ, and Cohen's d (Supplementary Tables S7–S8; Figs. S3–S4), and normalize meltwater chemistry to global riverine and marine baselines (Tables S3–S4). This integrative process based comparison (adapted from Hawkings et al.[2]) enables consistent evaluation of meltwater geochemistry across diverse glaciers, revealing how lithology, hydrology, and redox state govern TMs release, and how mountain glaciers vs polar system may diverge under warming climate driven changes[11]. These tools, adapted from the

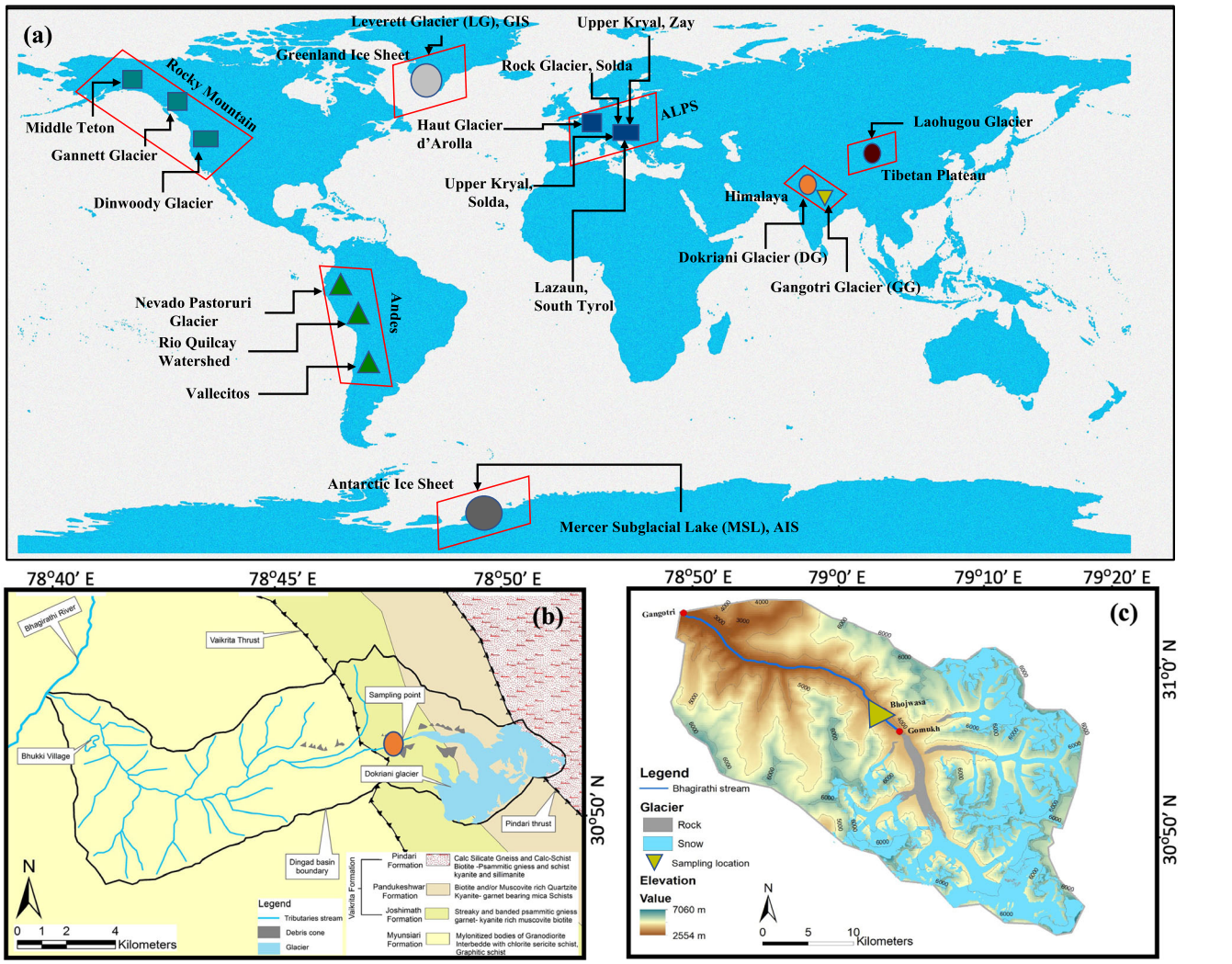

Fig. 1 | Location and site-level context of glacierized catchments included in this study. a Global distribution of the 14 mountain glaciers and 2 icesheet sites analyzed, spanning a wide range of latitudes, climatic zones, and lithologic settings. Sites are grouped by mountain belt or ice sheet province: Rocky Mountains (Middle Teton, Gannett, Dinwoody), Andes (Nevado Pastoruri, Rio Quilcay. Vallecitos, Argentina), Alps (Haut Glacier d'Arolla, Upper Kryal Solda, Upper Kryal Zay, Rock Glacier Solda and Lazaun/South Tyrol,), Himalaya (Gangotri, Dokriani), Tibetan Plateau (Laohugou Glacier), Greenland Ice Sheet (Leverett Glacier), and the Antarctic Ice Sheet (Mercer Subglacial Lake). Symbols differentiate major regions: squares = Rocky Mountains, triangles = Andes, big circles = ice sheet sites, and small circles = Himalaya/Tibetan (orange circle = Dokriani, yellow triangle = Gangotri, dark red circle = Laohugou). **b** Detailed basin map of Dokriani Glacier (Himalaya), showing its proglacial drainage network (blue lines), tributaries, and sampling location (orange circle). Bedrock geology is overlain (colors) based on regional formation mapping: Pandukeshwar Formation (metamorphics), Pandusar, Jhala, and other units (key to the right). Glacier margins (white) and snowfields (light blue) delineate accumulation and ablation zones. **c** Digital elevation model (DEM) of the Gangotri Glacier catchment, illustrating the longitudinal profile of the main proglacial channel (blue line) and the location of the Gangotri sampling site (yellow triangle).

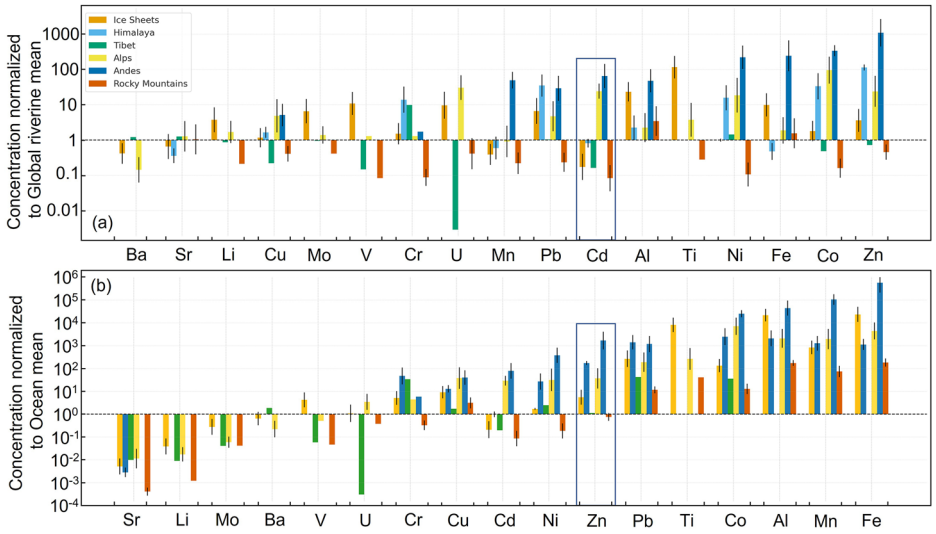

Fig. 2 | Normalized elemental concentrations in glacier and ice-sheet meltwaters relative to global river and ocean mean. a Site-level mean concentrations of TM normalized to the global riverine mean[39]. **b** The same elemental concentrations normalized to the global ocean mean[41]. Each symbol represents a glacierized catchment or ice-sheet outflow, grouped by region: Greenland Ice Sheet (LG, GIS) and Antarctic Ice Sheet (MSL, AIS) (Light orange color bar), Himalayan glaciers (Dokriani, Gangotri, Light Blue color bar), Andes glaciers (Dark Blue color bar), Tibetan Plateau glaciers (Green color Bar), Alps glaciers (Yellow color bar), and Rocky Mountain glaciers (Dark orange color bar). The horizontal black dashed line marks the global river (**a**) or ocean (**b**) mean. Values > 1 indicate enrichment relative to the reference mean, whereas values <1 indicate depletion. Supplementary Tables 3, 4 contains datasets used to generate the (**a**) and (**b**) respectively.

comparative framework developed by Hawkings et al.[2], enable a consistent evaluation of meltwater geochemistry across diverse glacier systems. This integrative approach enables process-based comparison of TMs export across diverse glacierized catchments, revealing how lithology, hydrology, and climate govern meltwater chemistry and how mountain and polar systems may diverge under accelerating cryospheric change[23].

Results and discussion

Meltwater TM concentrations and geochemical controls

Glacial meltwaters are emerging as significant, yet underappreciated sources of dissolved TMs to downstream aquatic systems, often exceeding those from polar ice sheets and non-glacial rivers in both concentration and variability[2,23]. Across the sixteen glacier-fed catchments in our dataset, TM concentrations span several orders of magnitude, underscoring the strong influence of local lithology, atmospheric deposition, and melt-season dynamics. Zn alone varies by nearly three orders of magnitude, from <1 μg L^{-1} in selected Tibetan Plateau sites to >1000 μg L^{-1} in the central Andes. Similarly wide ranges were also observed for Pb, Cu, Fe, Ni, and Cd (Supplementary Table S2). Such heterogeneity highlights the sensitivity of metal fluxes to both substrate and hydroclimate. Mountain ranges including the Himalaya, Alps, Andes, and Rocky Mountain consistently display elevated TM levels, each reflecting distinct geologic and climatic regimes. In the Himalaya, debris-covered glaciers (such as DG) accumulate higher TM concentrations, likely due to enhanced dust and aerosol deposition on stagnant debris layers, whereas clean-ice glaciers (such as GG) exhibit TM signatures dominated by subglacial weathering[24,25]. Lithology exerts a strong control on these patterns: carbonate bearing and sulfide rich bedrock enhances Zn, Ni, and Pb fluxes, consistent with sulfide oxidation coupled to carbonate buffering reactions. Superimposed on this geogenic baseline are seasonal melt pulses, especially during monsoon runoff, that transiently elevate metal loads. These peaks coincide with sharp increases in EFs, reflecting both intensified subglacial flushing and mobilization of deposited aerosols. In summary, dissolved TM concentrations in mountain glacier meltwater are not uniform but reflect a hierarchy of controls, i.e., lithology, hydrology, and atmospheric coupling that amplify geochemical contrasts among regions[20]. The following sections quantify these spatial patterns and explore their mechanistic underpinnings across different Cryospheric regimes.

Concentration variability in dissolved TMs in streams from 14 mountain glaciers show pronounced spatial variability, often exceeding those from polar ice sheets and global rivers by one to two orders of magnitude (Supplementary Table S2). Particularly notable are the datasets from Himalayan Mountain glaciers, where DG meltwater exhibit mean concentrations ranging from ~0.7 μg L^{-1} (Pb) up to ~77.7 μg L^{-1} (Zn). GG has mean concentrations from ~15.0 μg L^{-1} (Fe) to ~23.6 μg L^{-1} (Ni) (Supplementary Table S2). These values are striking when placed in a global context: Zn in DG and GG are ~129× and ~95× higher, respectively, than the global riverine mean of ~0.6 μg L^{-1}, while Pb concentrations exceed the global average (~0.08 μg L^{-1}) by factors of ~9 (DG) and ~61 (GG) (Fig. 2a; Supplementary Table S2). This degree of enrichment places Himalayan glaciers outflows near the upper limit of natural freshwater metal concentrations globally, emphasizing their disproportionate influence on regional biogeochemical cycling controlled through lithology. DG is underlain by calcsilicate and schist, whereas GG overlies granite schist interbedded with carbonate rich veins[26]. While carbonate horizons can partially buffer acidity, the dominant weathering process in both systems is sulfide oxidation, particularly of disseminated pyrite. This reaction releases protons, enhances metal solubility, and promotes the mobilization of Zn, Ni, Cu, and Fe in GG where carbonate buffering is limited. Comparable lithologic patterns occur globally. Proglacial streams on the Tibetan Plateau display very low TM concentrations (e.g., Zn ≈ 0.4 μg L^{-1}; Pb ≈ 0.1 μg L^{-1}; Cd ≈ 0.01 μg L^{-1}), while those in the Rocky Mountains are similarly low for most metals (Zn ≈ 0.3; Pb ≈ 0.02; Cd ≈ 0.01) but show a moderately higher Fe (≈4.6 μg L^{-1}). The European Alps exhibit still greater values (Zn ≈ 3.7; Cd ≈ 1.3; Pb ≈ 0.5; Cu ≈ 1.7; Fe ≈ 45 μg L^{-1}), and the Andes stand out with extreme enrichment (Zn ≈ 81; Cd ≈ 1.0; Pb ≈ 3.3; Cu ≈ 6.4; Fe ≈ 3049 μg L^{-1}). Non-parametric Mann–Whitney *U* tests show no statistically significant differences between mountain-glacier and ice sheet groups ($p > 0.05$ for all elements; Table S7; Section S3.2). However, the direction of the differences is consistent across independent metrics (U, Cohen's d, Cliff's δ; Tables S7–S8). Mountain glaciers tend to exhibit higher concentrations of chalcophile elements (Cd, Zn, Ni), while ice sheets display higher Fe and Cr, reflecting redox controlled mobilization under subglacial anoxia[27]. These results reinforce the interpretation that lithology and subglacial redox environment, govern the global distribution of TMs rather than climate zone.

Atmospheric deposition further amplifies TMs loading, particularly in regions downwind of major arid basins. Dust borne aerosols from Central Asia and the Tibetan Plateau deliver Zn, Pb, and other metals to snow and ice[25]. Surface snow data across north-western China show Zn between 0.09 and 1.36 μg L^{-1} [28]; snowpacks at Laohugou Glacier (LHG) and Qiyi Glacier average 1.3 μg L^{-1}, while those from Yuzhufeng and Miaoergou Glaciers record 0.5–0.9 μg L^{-1}. Even within single ranges, heterogeneity persists: Zn concentrations at Zhaosu (0.65 μg L^{-1}) and Keqikaer (0.24 μg L^{-1}) exceed those at Miaoergou (0.09 μg L^{-1}). These gradients reflect differences in dust source proximity and atmospheric circulation. In Himalayan catchments,

elevated Zn and Pb indicate mixed lithogenic and atmospheric origins[25,28]. Similar enrichment patterns occur in the Alps and Himalaya, where Fe, Zn, Cu, Ni, Cd, and Pb in glacial meltwaters exceed non-glacial riverine means by one to two orders of magnitude[22,29]. In the Ganges Basin, glacier melt contributes up to ~70 % of the dissolved Fe flux during ablation[30], illustrating the disproportionate influence of glacier derived TMs on regional river chemistry. Supraglacial snow and ice frequently exceed local crustal backgrounds for Zn and Pb, sourced from industrial emissions, fossil fuel combustion, and coal fly ash[25]. Seasonal melt pulses remobilize these surface stored metals, producing short-lived but intense TM export events that coincide with hydrological peaks[31].

Our analysis centers on proglacial outlet waters, where lithologic and atmospheric inputs converge, providing an integrated and ecologically relevant measure of TM export to downstream environments (Supplementary Table S2). This dual imprint (geogenic and atmospheric) highlights the need for TM risk frameworks that incorporate both bedrock weathering and atmospheric deposition pathways when assessing glacier contributions to regional water quality and ecosystem health.

Enrichment patterns: mountain glaciers versus ice sheets

Global comparisons reveal a consistent divergence in TMs enrichment between mountain glaciers and polar ice sheets (Fig. 2). Although meltwaters from all glacier types exceed global riverine means, the magnitude and direction of enrichment vary systematically with region, element, and bedrock composition[28,32,33]. Chalcophile metals (Zn, Co, Ni, and Pb) show the clearest contrast: concentrations in mountain glacier meltwaters (e.g., Gangotri and Dokriani in the Himalaya; Arolla and Lazaun in the Alps; Pastoruri in the Andes; Laohugou on the Tibetan Plateau; Dinwoody and Middle Teton in the Rocky Mountains) consistently exceed those in ice sheet outlets such as Leverett Glacier (GIS). Zn exhibits the most coherent signal, with mountain glaciers exceeding ice-sheet values by one to two orders of magnitude, reflecting vigorous oxidative weathering and rapid subglacial ventilation. By contrast, Cr shows region specific enrichment tied to mafic and ultramafic substrates in Himalayan and Tibetan catchments[11,20,21]. These geographic trends underscore the primacy of bedrock geochemistry in governing TM export across cryospheric regimes[5,11,23].

Not all elements follow uniform behavior. Ba and Sr typically lie below global riverine means, suggesting widespread depletion except in isolated basins (Fig. 2a). Their subdued signal reflects low crustal abundance and removal by adsorption or co-precipitation with Fe–Mn oxyhydroxides during subglacial transit[2,18,34]. In contrast, Cd, Mn, Fe, and Cu display mixed responses: strong enrichment in some catchments most notably the Andes but near-background values elsewhere. Cd exceeds 100 μg L^{-1} in Vallecitos (Argentina) and ~24 μg L^{-1} in Alpine streams, yet approaches the riverine mean in the Himalaya. Fe reaches extreme levels in the Andes (~3 mg L^{-1}) and remains high in the Antarctic Mercer Subglacial Lake (~6 μg L^{-1}), reflecting sulfide oxidation under low-oxygen conditions coupled with limited secondary mineral sequestration[2,16,35]. These spatial divergences confirm that TM mobilization beneath glaciers is not governed by uniform depletion but by the interplay among bedrock composition, redox microenvironments, and drainage connectivity challenging the long-held assumption that cold regions export negligible metal fluxes[15,20].

Distinct weathering regimes leave diagnostic TM fingerprints. In the Himalaya, sulfide oxidation within metamorphic bedrock mobilizes Zn, Ni, and Co, producing higher concentrations in GG relative to ice sheet sites[8]. GG's sulfide-bearing schists release Ni, Co, and Zn, whereas DG's schists host Cr-rich minerals such as biotite and amphiboles[22,23]. Conversely, Mn is uniformly suppressed across ~85 % of sites (<5 μg L^{-1}), except in an Andes location (46.83 μg L^{-1}), likely due to sorption onto Fe(III) oxyhydroxides[2]. These patterns show that while redox driven weathering spikes Zn, Cu, and Ni in sulfide rich terrains, adsorption and co precipitation processes constrain Mn yielding site specific TM fingerprints. The consistently high enrichment of certain metals, particularly Zn, suggests contributions beyond rock weathering alone. In regions like DG & GG, Alps, and Rocky Mountain, Zn concentrations frequently exceed crustal normalized values by >100–1000× (Fig. 2). Such extreme Zn level point to inputs beyond natural rock weathering. They could reflect unusual Zn rich bedrock lithologies or atmospheric deposition of pollutants (e.g., Zn from smelter emissions, coal fly ash) that drive Zn concentrations far above crustal supply[25]. Additionally, release of TMs accumulated in older glacier ice (which may contain higher impurity loads from past atmospheric deposition) can cause pulses of TMs in meltwater[2,35]. The varied enrichment patterns we observe likely reflect a combination of these processes: natural weathering of local bedrock plus external inputs (atmospheric or legacy contaminants in ice)[25]. Distinguishing these sources will require detailed isotope or speciation studies[17,25,33], but the broad patterns indicate mountain glaciers have a propensity for higher TMs release (especially transition metals) relative to polar ice environments.

When normalized to open ocean mean concentrations, TMs in glacier meltwaters reveal globally coherent enrichment patterns (Fig. 2b). Concentrations of biologically essential elements including Mn, Ni, Cu, Co, Fe, and Al are consistently elevated across high-relief glacierized regions such as the Himalaya, Alps, Andes, and Rocky Mountains. This pattern suggests that glaciers serve as important sources of micronutrients to downstream marine ecosystems. These trends are statistically robust: Kruskal Wallis tests show significant inter-regional differences for Zn ($H = 82.6$, $p < 10^{-13}$), Ni ($H = 55.3$, $p < 10^{-9}$), and Cu ($H = 47.8$, $p < 10^{-7}$), with pairwise comparisons consistent with higher TMs enrichment in the Himalaya and Andes relative to polar basins. Alps catchments such as Upper Kryal, Zay, Upper Kryal, Solda, Lazaun display elevated Zn, Al, Fe and Ni, a signature likely tied to steep topographic gradients and metal bearing metamorphic bedrock that promotes rapid leaching. Rocky Mountain glaciers (e.g., Dinwoody, Middle Teton) show comparable enrichment patterns, underscoring the combined influence of local mineralogy and subglacial hydrology. By contrast, Tibetan catchments (e.g., Laohugou) are marked by high Pb, Co, and Cr but only moderate Cu and Ni, with Cd concentrations remaining persistently low, consistent with silicate-dominated substrates and reduced hydrologic flushing under arid conditions. In contrast, metals such as Mo, Sr and Li show consistent depletion across glacier fed waters relative to open ocean mean concentrations, indicating either limited availability in glacial source rocks or removal during transit via processes such as adsorption onto mineral surfaces, incorporation into secondary precipitates, or co precipitation with carbonates and oxides before reaching downstream waters[27,36,37]. Glacier meltwaters carry elemental signatures that diverge sharply from open ocean mean concentrations, reflecting lithological diversity, weathering pathways, and hydrological routing. In the Himalaya, sulfide oxidation mobilizes Zn, Fe, Al and Co, while anthropogenic deposition elevates Zn further[36]. Yet, as Hawkings et al.[2] emphasized, glaciers act as selective suppliers: they enrich the ocean in bioavailable micronutrients such as Fe but contribute little of other TMs owing to lithological scarcity or subglacial removal. With accelerating mountain glacier retreat, these imbalanced fluxes are poised to intensify, reshaping nutrient limitation regimes and altering marine carbon cycling from coastal margins to the open ocean[2,27,30].

Mobility patterns: mountain glaciers versus ice sheets

Across all surveyed basins, both mountain glaciers and ice sheet outlets display consistently elevated MI for elements with high aqueous solubility and weak mineral binding, including Fe, Co, Zn, U, Cr, Ni, and Pb (Fig. 3). This convergence indicates that irrespective of geographic setting or glacial type such metals are efficiently mobilized during meltwater generation. The magnitude of mobility, however, diverges sharply between settings. Mountain glaciers exhibit systematically higher MI values for several TMs, particularly Zn, Cu, Ni, and Cd, relative to ice sheets (Fig. 3; Supplementary Table S5). For instance, Cd reaches MI values exceeding 240 in Upper Kryal, Solda, 10 in Haut Glacier d' Arolla, 110 in Upper Kryal, Zay (Alps), 3.1 in DG (Himalaya), and 6.04 in Gannett Glacier (Rocky Mountain Glaciers), yet remains nearly immobile (MI < 0.15) in LG, GIS, and MSL, AIS. Zn shows the same pattern, with MI spanning 1–203 in Alps, 5–17 in Rocky Mountain Glaciers, and exceptionally high values in Himalayan basins such as DG

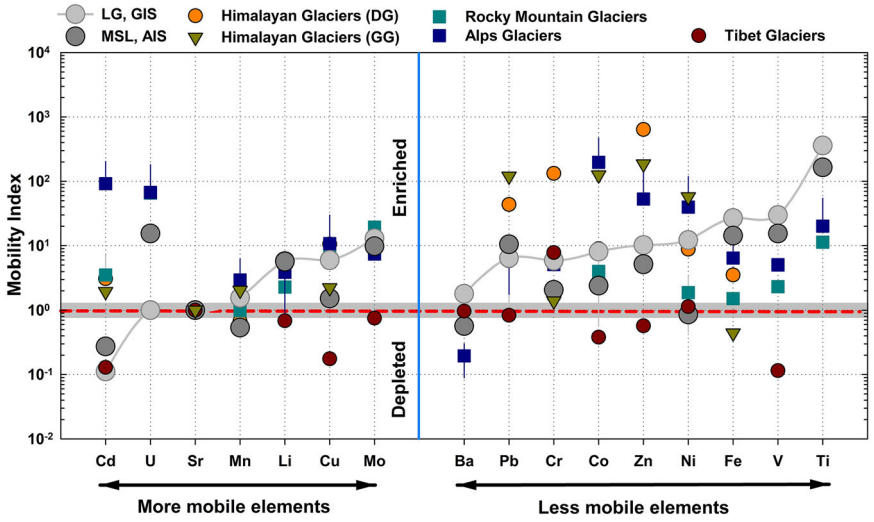

Fig. 3 | Normalized mobility index (MI) of TM in the dissolved fraction of glacier meltwaters. The MI quantifies the relative mobility of each element in the < 0.45 µm dissolved fraction by normalizing meltwater concentrations first to their abundance in the upper continental crust[44] and then to strontium (Sr = 1). Each symbol represents the MI for a glacierized catchment or ice-sheet outflow, color-coded by region: Greenland Ice Sheet (LG, GIS) and Antarctic Ice Sheet (MSL, AIS) (gray circles), Himalayan glaciers (Dokriani, orange circles; Gangotri, gray invert triangles), Tibetan Plateau glaciers (brown circles), Alps glaciers (dark blue squares), and Rocky Mountain glaciers (cyan squares). Metals are arranged from more mobile (left) to less mobile (right) based on their average behavior in global river systems[44]. The horizontal red line marks the global riverine baseline (Sr-normalized MI = 1); the shaded band shows the ±1 SD range, values above this line indicate enhanced mobility relative to crustal abundance, whereas values below indicate relative depletion. The datasets used to generate this figure are provided in Supplementary Table 5.

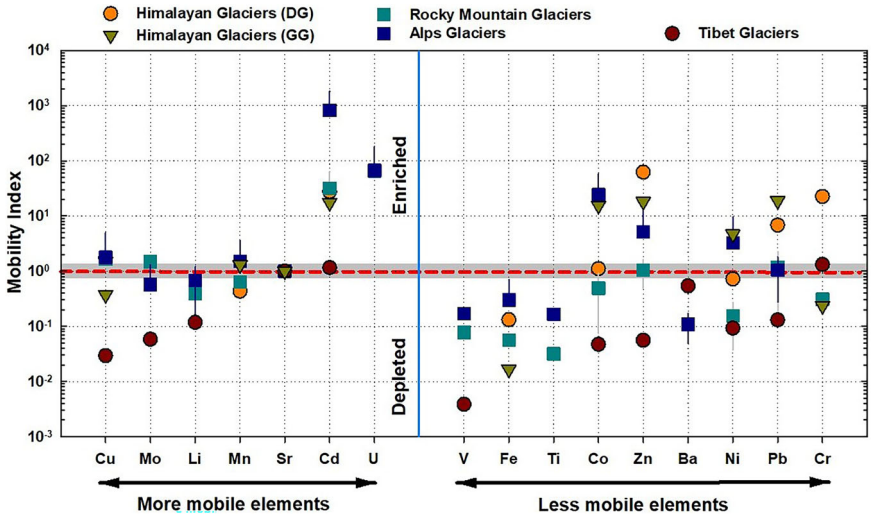

Fig. 4 | Normalized mobility index (MI) of TM in mountain glacier meltwaters relative to ice-sheet meltwaters. The MI quantifies the relative mobility of each element in the < 0.45 µm dissolved fraction by normalizing mountain glacier meltwater concentrations first to their abundance in the upper continental crust[44] and then to the mean concentration observed in ice-sheet meltwaters (Greenland and Antarctic Ice Sheets). Each symbol represents a mountain glacier site grouped by region: Himalayan glaciers (Dokriani, orange circles; Gangotri, Green triangles), Tibetan Plateau glaciers (dark red circles), Alps glaciers (dark blue squares), and Rocky Mountain glaciers (cyan squares). Metals are arranged from more mobile (left) to less mobile (right) based on their average behavior in global river systems[39]. The horizontal red line marks the baseline of ice-sheet concentrations (MI = 1); the shaded band shows the ± 1 SD range, values above this line indicate metals that are more mobile in mountain glacier meltwaters relative to ice sheets, whereas values below indicate relative depletion. The datasets used to generate this figure are provided in Supplementary Table 6.

(637) and GG (186), compared to a narrow 5–10 range in ice-sheet systems. These directional contrasts were consistent across non-parametric tests but did not reach statistical significance due to small ice sheet sample size (Table S7). This pronounced divergence reflects the steeper gradients, faster subglacial water transit, and sulfide rich lithologies characteristic of mountain glacier catchments, which together enhance metal weathering and release[11]. As a result, mountain glaciers act as disproportionately powerful engines of TMs mobilization on a global scale, despite occupying only a fraction of the area of polar ice sheets[2].

Several TMs including Mn, Ba and Fe show uniformly low mobility across glacier systems, reflecting either scarcity in source lithologies or strong retention via adsorption and co-precipitation[27] (Fig. 3). The Laohugou Glacier in Tibet illustrates this clearly, with consistently suppressed MIs for many TMs, likely due to its specific lithologic context and conservative weathering regime (Figs. 3, 4, Supplementary Tables S5, 6). Fe itself provides a striking contrast: Fe mobility is typically lower in mountain glaciers than in ice sheets. This inversion arises because polar ice sheets host extensive subglacial sediments with longer water residence times, enhancing reductive dissolution of Fe-bearing phases and sustaining higher Fe export[6]. Laboratory leaching experiments reinforce this interpretation: Fe-oxyhydroxide coatings and secondary carbonate phases can scavenge TMs from solution within hours to days at near neutral pH[23,27], producing strong local retention. By contrast, alpine catchments flush rapidly through steep drainage networks, where oxygenation promotes precipitation of Fe-oxyhydroxides that sequester dissolved Fe before export[2,11,31]. This explains why Fe concentrations are consistently elevated in ice sheet meltwater relative to mountain glaciers, despite the latter experiencing more vigorous sulfide oxidation.

Relative comparisons across TMs highlight systematic enrichment rather than depletion (Fig. 4, Supplementary Table S6). Cd is consistently more mobile in mountain glaciers than ice sheets, while Cu shows strong regional variation: Himalayan glaciers yield MI values of 0.4–1.8, the Alps 0.01–7.5, the Rocky Mountains 0.21–3.6, but Laohugou Glacier remains anomalously low (MI ≈ 0.03). These divergences reflect local bedrock Cu

content, the availability of organic ligands, and redox conditions[6,24]. Dissolution tests confirm that oxidative leaching of Cu-bearing sulfides can release up to ~50% of particulate Cu within 48 h under acidic, oxic conditions[16]. Notably, Cd and Zn concentrations are systematically higher in most mountain glaciers than in any icesheet samples, underscoring the role of high relief catchments in amplifying TMs solubility. Flow through experiments further show that high discharge events mobilize Cu, Zn, and Ni through sulfide oxidation and desorption from particle surfaces mechanisms intensified in dynamic alpine systems[2,14]. Shallow ice, thin debris mantles, and vigorous meltwater flushing enhance rock water contact and oxygen delivery, driving oxidative weathering of metal sulfides and dissolution of trace phases[9,13,14]. While these patterns are robust, caveats remain: uneven spatial sampling, detection-limit variability, and incomplete normalization to discharge or grain size could bias comparisons. These limitations do not overturn the regional signal but highlight the urgent need for standardized, cross system datasets to refine global inter-glacier assessments.

Debris cover on glaciers further amplifies TMs release. A thick supraglacial debris layer, as on lower Gangotri, increases rock water interaction by routing melt through debris and subglacial sediments. Debris also retains heat, prolonging subglacial drainage and chemical weathering. Our data show debris rich Himalayan glaciers (GG, Upper Kryal, Solda) yielding higher dissolved loads for certain metals than debris poor glaciers (Laohugou). For example, the Upper Kryal, Solda streams in the Alps shows extraordinarily high Cd mobility (MI ~ 2166) and GG's high Pb (18.8) and Cd (17.5) mobilities. These extremes likely result from more intense subglacial weathering enhanced by insulating debris cover. Debris can also acidify meltwater through oxidation of sulfide bearing minerals in the sediments, further increasing metal solubility. Studies indeed find subglacial outflows from debris covered glaciers carry elevated metal concentrations due to prolonged water rock contact[8,26]. Additionally, debris fosters microbial communities that mediate weathering reactions and metal cycling[37], potentially releasing metals like Fe and Mn through microbial oxidation.

Climate warming is amplifying these disparities. As global glacier mass loss have more than doubled since the 1980s[3], our 16 site synthesis reveals that, on an area normalized basis, mountain glaciers now release up to 6 fold more Zn, 8-fold more Cu, 19-fold more Pb, and an extraordinary 90 fold more Cd than ice sheets (Fig. 4; Supplementary Table S6). As warming shifts melt onset earlier and accelerates seasonal discharge, mountain glaciers are emerging as short-lived biogeochemical hotspots. Pulsed TM fluxes particularly in early summer are likely to increase, compounding downstream risks and benefits. While Cd and Zn may transiently fertilize oligotrophic rivers and nearshore zones[38], Cd and Pb concentrations may intermittently approach or exceed toxicity thresholds in low-alkalinity headwaters[18]. Yet this pulse is transient. The eventual disappearance of small, high relief glaciers currently the most chemically reactive will curtail localized TM sources, triggering a long term decline in glacially sourced micronutrients and pollutants[10].

Taken together, our synthesis shows that glacier morphology, as much as geochemistry, governs the scale of TMs export. Small, steep mountain glaciers act as chemical amplifiers, mobilizing metals rapidly through intense erosion, minimal debris shielding, and efficient meltwater flushing. By contrast, the vast ice sheets with predominantly cold based sectors and sluggish subglacial drainage retain much of their metal load, muting downstream fluxes despite their size. Across both systems, however, the relative mobility of elements such as Zn, Cd, and Ni reflects common weathering susceptibilities, dictated by redox reactivity and mineral solubility[23]. These contrasts not only redefine the global footprint of glacial metal fluxes under climate warming, but also frame the cryosphere as both a transient pulse and a diminishing reservoir of critical elements.

Downstream implications

Glaciers are not merely melting, they are metabolizing landscapes, transforming rock and atmospheric inputs into chemical exports that cascade through river systems. As mountain glaciers retreat, they release concentrated pulses of TMs into headwaters, transmitting chemical legacies that can either fertilize life or poison it far downstream.

On the positive side, elements such as Fe, Zn, and Co act as essential micronutrients in oligotrophic alpine and polar waters[2]. High Fe fluxes from ice sheets can stimulate phytoplankton growth in nutrient-poor lakes and coastal oceans, enhancing biological carbon uptake[1,28]. Similarly, elevated Zn and Co concentrations in mountain glacier meltwaters can alleviate micronutrient limitation for algae and bacteria, serving as cofactors in key enzymatic pathways. Early season melt pulses, when runoff is most concentrated, may thus provide transient nutrient subsidies that sustain productivity in otherwise nutrient starved headwaters[37]. Yet this nutrient boon carries a toxic trade-off. Elevated TM levels particularly Pb and Cd even at microgram-per-liter concentrations, can bioaccumulate and magnify through aquatic food webs, threatening fisheries, wildlife, and human water supplies[27,38]. Our 14 site synthesis shows that mountain glacier outflows export up to six times more Zn, eight times more Cu, nineteen times more Pb, and ninety times more Cd per unit area than ice sheet outlets (Fig. 4; Supplementary Tables S5–S6). In sulfide-rich catchments of the Himalaya and Alps, Cd concentrations reach 0.1–0.5 μg L^{-1} below the WHO drinking water guideline of 3 μg L^{-1} but approaching the US EPA chronic aquatic life threshold (0.25 μg L^{-1}) whereas ice sheet rivers remain consistently <0.1 μg L^{-1}. Pb follows a similar pattern: levels up to 4.9 μg L^{-1} in the Himalaya, 4.3 μg L^{-1} in the Rockies, and 0.5 μg L^{-1} in the Alps already exceed the US EPA chronic aquatic-life limit (0.25 μg L^{-1}) for soft waters[35,39], despite being largely derived from natural mineral weathering. Seasonal timing amplifies these contrasts: during monsoon and early-summer melt peaks, TM concentrations surge (Supplementary Fig. S1), delivering short-lived chemical shocks that can either stimulate or stress fragile headwater ecosystems depending on buffering capacity and biological demand.

These findings call for integrated ecological and hydrological monitoring in glacierized regions. As melt regimes intensify under warming, so will fertilization toxicity trade-offs[2,18]. Monitoring efforts should target both essential micronutrients and hazardous TMs, with seasonal and interannual resolution to capture emerging risks and tipping points[2]. Multiyear datasets will be vital to forecast water quality dynamics, support adaptive ecosystem management, and inform early warning systems for vulnerable downstream users. On a global scale, increasing glacier TM fluxes could modulate ocean nutrient balances and carbon cycling particularly via Fe stimulated productivity in the Southern Ocean and Indian Ocean margins[34]. Yet the benefits of such fertilization must be weighed against pollutant co-fluxes that threaten food safety, fisheries, and water security.

In sum, the chemical signatures of glacier meltwater are not passive reflections of retreat but active agents shaping riverine and marine systems. Whether these changes manifest as fertilization or contamination will depend on glacier type, lithology, climate trajectory and the speed at which we respond[2,23]. Because glacier melt and weathering are physically irreversible, direct remediation at the source is not possible. However, process based strategies can attenuate downstream impacts. Natural attenuation zones such as proglacial wetlands and floodplains can sequester or transform mobilized metals, while engineered interventions (e.g., passive treatment systems, sorbent materials) may be targeted at discharge hotspots. Crucially, real-time hydrochemical monitoring offers an adaptive lever linking seasonal melt dynamics with early detection of toxic fluxes[23]. Thus, while metal release is an inherent outcome of glacial retreat, its propagation through river networks remains a tractable point of control[28].

Conclusions and forward outlook

This study provides a global synthesis of the dissolved TMs behavior across glacierized environments, demonstrating that both mountain glaciers and ice sheets release meltwaters enriched in specific metals relative to global riverine and marine baselines, but through distinct geochemical pathways. By integrating meltwater datasets from 14 mountain glaciers and 2 ice sheets, we show that glacial chemistry is highly context-dependent: mountain glaciers enrich both essential and toxic TMs to levels far above

global riverine and marine benchmarks, whereas ice-sheet outflows remain comparatively dilute. TMs such as Cd, Cu, and Zn exhibit particularly high mobility in mountain settings, recognizing these glacier-specific controls are essential for predicting ecological trajectories of weathering. The novelty of this work lies in demonstrating, across diverse regions from High Asia to the Andes, Alps, and Rockies that glacier type, not just geochemistry, governs TM mobilization and export intensity. Our findings reposition mountain glaciers as globally significant yet vulnerable suppliers of critical elements, with implications extending beyond toxicity to nutrient delivery, food webs, and freshwater quality. As climate change accelerates glacier retreat, mountain catchments will likely undergo the sharpest chemical perturbations, with local communities facing both beneficial nutrient influxes and heightened pollution risks. Recognizing these glacier-specific controls is essential for predicting ecological trajectories and for incorporating the cryosphere's chemical imprint into future biogeochemical and climate frameworks.

Methods overview and data linkage

Study sites and sample collection

We investigated dissolved TMs in meltwater from 16 glacierized catchments worldwide: 14 mountain glaciers and 2 ice-sheet outlet systems (Supplementary Tables S2–S6). The mountain sites span diverse geologic and climatic settings, including the central Himalaya (Dokriani and Gangotri Glaciers), the Tibetan Plateau (Laohugou Glacier), the European Alps (Haut Glacier d'Arolla, Lazaun Glacier, two Upper Kryal streams, a rock-glacier outflow in Solda Valley, and others), the American Rocky Mountains (Dinwoody, Gannett, Middle Teton Glaciers), and the Andes (Rio Quilcay basin and Nevado Pastoruri region in Peru, Vallecitos in Argentina). For polar comparison, we included meltwater from Leverett Glacier (a land-terminating outlet of the Greenland Ice Sheet) and discharge from Mercer Subglacial Lake beneath the West Antarctic Ice Sheet. Supplementary Table S2 summarizes the site locations, sampling periods, and data sources. the Himalayan sites (Dokriani and Gangotri), we collected samples directly as part of this study (2015–2019 campaigns) using ultra-clean techniques. For the other sites, we compiled high quality published datasets (all originally filtered to <0.45 μm and acidified for dissolved metal analysis) to ensure consistency. Field sampling at each site targeted summer melt seasons when glacial runoff is highest, with samples taken near the glacier terminus or proglacial outlet. Water was passed through pre-rinsed 0.45 μm filters into acid washed polyethylene bottles, then acidified to pH < 2 with ultrapure HNO_3 to prevent metal adsorption. Strict blank handling protocols were followed: field blanks (exposed to sampling kits) and procedural blanks (lab ultrapure water filtered and acidified) were analyzed alongside samples to check for any contamination. In our own sampling, we applied blank corrections by subtracting measured blank values from sample concentrations (these corrections were generally minor, on the order of <0.01 μg L^{-1} for most TMs, i.e., well below typical concentrations). All sample bottles were kept chilled and double bagged during transport, then stored at 4 °C until analysis. More details of field sampling methods are outlined in section S1.2.

Analytical methods

Dissolved metal concentrations were determined by high resolution inductively coupled plasma mass spectrometry (ICP-MS). For our new Himalayan samples, we utilized a Thermo Fisher ICP-MS in low flow clean laboratory conditions. The instrument was calibrated with multi element standard solutions covering the range of expected concentrations, and internal standards (e.g., indium, rhenium) were used to correct for drift and matrix effects. External quality assurance was provided by analyzing certified reference waters (e.g., NIST TMs in water) recoveries were within 90–110% for all reported elements. For compiled literature data, original sources used similar ICP-MS techniques; we cross-validated a subset of overlapping measurements between studies and found agreement within analytical uncertainties. Detection limits (3× signal-to-noise) were typically in the tens of ng L^{-1} for elements like Cd, Co, Pb, and ~0.1–1 μg L^{-1} for more abundant elements like Fe, Al, Zn[40]. All concentrations were recorded in μg L^{-1}. Where datasets spanned multiple years or seasons, we used mean or median values per site to represent typical meltwater chemistry, so that each glacier site is treated as one data point in comparative analyses. This averaging minimizes bias from short-term fluctuations (e.g., diurnal cycles or rain events) and focuses on sustained differences between sites. Details are also presented in Section S1.4.

Chemometric metrics

Enrichment factor (EF) calculation. To assess the degree of metal enrichment beyond natural crustal sources, we calculated an EF for each element at each site. EF is defined as the ratio of a metal's concentration in the meltwater to its expected concentration if derived solely from average crustal weathering. In practice, we computed:

$$\mathrm{EF}(\mathrm{X}) = \frac{\left(\frac{\mathrm{X}}{\mathrm{Al}}\right)\text{meltwater}}{\left(\frac{\mathrm{X}}{\mathrm{Al}}\right)\text{Upper Continental Crust}}$$

Using Al as a conservative reference element (or Fe, when appropriate)[41,42]. EF values near 1 indicate a crustal origin, while EF > 1 suggests enrichment from external sources (e.g., anthropogenic or unique lithologies)[42]. We interpret EF values 0.5–1.5 as no significant enrichment or depletion, 1.5–10 as moderate enrichment (possibly enhanced weathering or minor pollution input), and >10 as high enrichment likely requiring an anthropogenic source[25]. Uncertainty in EF arises from natural crustal composition variability, but the metric provides a useful first order source indication.

Mobility index calculation. We also used Mobility Index (MI) the relative mobility of different elements under glacial weathering conditions, independent of their absolute concentrations. The concept of MI builds on normalizing metal concentrations to average UCC abundance for each element[43], yielding a rock-normalized concentration. We then normalized these values to strontium (Sr), an element with relatively high mobility during weathering in our study area. Sr was chosen because it is a highly mobile, abundant alkaline earth element that is readily released by weathering of common minerals (carbonates, plagioclase) and is not strongly affected by redox or biological uptake in these systems. By dividing by the Sr ratio, we set a baseline of "overall solute yield" against which other elements are compared. We divided the TM_{norm} by the Sr concentration (μg L^{-1}) for each sample, resulting in an initial rock/solution ratio for each metal ($TM_{rock/solution}$). This two-step normalization (to UCC and to Sr) reduces biases from site-to-site lithological differences and total weathering intensity, honing in on the intrinsic mobility of each element in the glacial environment. Since the method assumes a constant Sr concentration of 1, we calculated a factor by averaging the rock/solution ratio for Sr across all samples. Compared to Na, Sr exhibits higher mobility during weathering. This makes Sr a more suitable normalizer for assessing the release of TMs from rock in our study. Na, on the other hand, may be more susceptible to geochemical processes that can alter its concentration in natural waters, potentially distorting the MI calculations[2]. While Sr normalization has limitations, such as potential sensitivity to pH variations, it offers a more accurate representation of elemental mobility in our specific study area. By accounting for the influence of rock type and geochemical processes, Sr normalization provides a more robust approach to assessing trace element release from glaciers. The MI for element X is thus:

$$\mathrm{MI}_{\mathrm{X}} = \frac{(\mathrm{X}/\mathrm{UCCx})}{(\mathrm{Sr}/\mathrm{UCCSr})}$$

so that MI > 1 indicates X is more mobile (released readily relative to Sr) and MI < 1 indicates less mobile (retained in solid phase relative to Sr). While Sr itself can be sensitive to carbonate weathering and pH, this two-

step normalization (to UCC and to Sr) accounts for lithological differences and allows comparison of elemental mobility across sites[2].

Statistical analysis. To quantify geochemical contrasts between glacier types, we applied a suite of non-parametric tests designed for small, heterogeneous datasets. Dissolved TM concentrations from 14 mountain-glacier sites and 2 ice-sheet outlets were compared using the two-sided Mann–Whitney *U* test, a rank-based approach robust to non-normal distributions and unequal group sizes. Analyses were restricted to metals with sufficient analytical coverage (Zn, Cu, Cd, Ni, Pb, Fe, and Cr) ensuring meaningful inference from site-level medians that minimize bias from hydrological outliers (Supplementary Table S7). Detailed statistical results are presented in the supplementary files.

Given the small and unbalanced sample sizes, we emphasized effect-size metrics as more informative indicators of contrast magnitude. Both Cohen's d (standardized mean difference) and Cliff's δ (a non-parametric measure of stochastic dominance) were calculated for each element (Supplementary Table S8; Fig. S4). The detailed information and formulas are provided in supplementary file section S3.

Data availability and visualization. All datasets underlying this analysis including raw concentration data, calculated EF, MI, and statistical outputs are provided in the Supplementary Information (Tables S1–S8; Figs. S1–S4). Results presented as Figs. 2–4, EF1 were generated using Sigmaplot version 15. Each plotted data point represents site-level mean concentrations ($n = 14$ mountain glacier, $n = 2$ icesheet), with error bars denoting 95% bootstrap confidence intervals. All statistical code, plotting scripts, and data pre-processing workflows are available upon request from the corresponding author. The analytical framework adheres to Nature statistical standards, emphasizing transparent reporting, reproducible computation, and physically interpretable metrics.

Reporting summary

Further information on research design is available in the Nature Portfolio Reporting Summary linked to this article.

Data availability

Datasets generated and analyzed during the current study are openly available in "Zenodo" at https://zenodo.org/records/17660757.

Received: 28 March 2025; Accepted: 21 November 2025;
Published online: 28 February 2026

References

1. Wadham, J. L. et al. Biogeochemical weathering under ice: size matters. *Glob. Biogeochem. Cycles* **24**, GB3025 (2010).
2. Hawkings, J. R. et al. Enhanced TM mobilization by Earth's ice sheets. *Proc. Natl. Acad. Sci. USA* **117**, 31648–31659 (2020).
3. Zemp, M. et al. Global glacier mass changes and their contributions to sea-level rise from 1961 to 2016. *Nature* **568**, 382–386 (2019).
4. Maurer, J. M., Schaefer, J. M., Rupper, S. & Corley, A. Acceleration of ice loss across the Himalayas over the past 40 years. *Sci. Adv.* **5**, eaav7266 (2019).
5. Hugonnet, R. et al. Accelerated global glacier mass loss in the early twenty-first century. *Nature* **592**, 726–731 (2021).
6. Kendrick, M., Yang, F., Olson, C. L. & Shelobolina, E. S. Biogeochemical controls on the mobility of arsenic and selenium in a coal mining region. *Environ. Sci. Technol.* **52**, 10434–10443 (2018).
7. Twining, B. S. & Baines, S. B. The trace metal composition of marine phytoplankton. *Annu. Rev. Mar. Sci.* **5**, 191–215 (2013).
8. Ferguson, R. J. The transport of sediments and heavy metals by the Fraser River. *Water Pollut. Res. J. Can.* **25**, 1–22 (1990).
9. Gao, Y., Arimoto, R., Zhou, X. & Chen, T. TM solubility in Asian dust and its impact on the ocean biogeochemistry: a review. *J. Geophys. Res. Atmos.* **116**, D23 (2011).
10. Liu, G. et al. Spatial and temporal variations of TM in atmospheric wet deposition in the Nam Co basin, central Tibetan Plateau. *Sci. Total Environ.* **758**, 143654 (2021).
11. Dong, Z. et al. Temporal and diurnal analysis of trace metals in the Cryospheric water at remote Laohugou basin in northeast Tibetan Plateau. *Chemosphere* **29**, 386–398 (2017).
12. Brighenti, S. et al. After the peak water: the increasing influence of rock glaciers on alpine river systems. *Hydrol. Process* **33**, 2804–2823 (2019).
13. Delpero, M. et al. Spatio-temporal variability of isotopic and chemical tracers in high-elevation water sources, Eastern European Alps. *J. Hydrol*. **662**, 133914 (2025).
14. Mitchell, A. C. & Brown, G. H. Diurnal hydrological—physicochemical controls and sampling methods for minor and TM in an Alpine glacial hydrological system. *J. Hydrol.* **332**, 123–143 (2007).
15. Brighenti, S. et al. Factors controlling the water quality of rock glacier springs in European and American mountain ranges. *Sci. Total Environ.* **953**, 175706 (2024).
16. Santofimia, E. et al. Acid rock drainage in Nevado Pastoruri glacier area (Huascarán National Park, Perú): hydrochemical and mineralogical characterization and associated environmental implications. *Environ. Sci. Pollut. Res.* **24**, 25243–25259 (2017).
17. Fortner, K. S. et al. Elevated stream trace and minor element concentrations in the foreland of receding tropical glaciers. *Appl. Geochem.* **26**, 1792–1801 (2011).
18. Carling, T. G., Rupper, S. B., Fernandez, D. P., Tingey, D. G. & Harrison, C. B. Effect of atmospheric deposition and weathering on TM concentrations in glacial meltwater at Grand Teton National Park, Wyoming, USA. *Arct., Antarct. Alp. Res.* **49**, 427–440 (2017).
19. Barkdull, N. S. et al. Glaciers control the hydrogeochemistry of proglacial streams during late summer in the Wind River Range, Wyoming, United States. *Front. Earth Sci.* **9**, 727575 (2021).
20. Sundriyal, S., Shukla, T., Tripathee, L. & Dobhal, D. P. Natural versus anthropogenic influence on Trace elemnts concentration in precipitation at Dokriani Glacier, central Himalaya, India. *Environ. Sci. Pollut. Res.* **27**, 3462–3472 (2020).
21. Sundriyal, S. et al. Controls of lithology and climate over chemical weathering trends: New insights from the precipitation-dominated Dokriani glacier, central Himalaya, India. *J. Glaciol.* **70**, 1–13 (2024).
22. Li, X. et al. Diurnal dynamics of minor and TM in stream water draining Dongkemadi Glacier on the Tibetan Plateau and its environmental implications. *J. Hydrol.* **541**, 1104–1118 (2016).
23. Hawkings, J. R., Wadham, J. L., Tranter, M. & Raiswell, R. The biogeochemistry of high-latitude glacial ecosystems. *Nat. Geosci.* **8**, 64–71 (2015).
24. Shukla, T., Sundriyal, S., Stachnik, L. & Mehta, M. Carbonate and silicate weathering in glacial environments and its relation to atmospheric CO_2 cycling in the Himalaya. *Ann. Glaciol.* **59**, 159–170 (2018).
25. Kang, S. et al. Insight into spatial and seasonal variations of elemental composition in Mt. Everest (Qomolangma) snow/firn. *Atmos. Environ.* **41**, 7208–7218 (2007).
26. Rogora, M. et al. Evaluating water quality of rock glacier outflows in the Western Alps, Italy: a regional perspective. *Environ. Monit. Assess.* **196**, 1100 (2024).
27. Statham, P. J., Skidmore, M. L. & Tranter, M. Inputs of glacially derived dissolved and colloidal iron to the coastal ocean and implications for primary productivity. *Glob. Biogeochem. Cycles* **22**, GB3013 (2008).
28. Wei, T. et al. Insight into atmospheric deposition and contamination of toxic zinc in remote glacier regions of Northwestern China. *Appl. Geochem.* **153**, 105683 (2023).
29. IPCC. *Special Report on the Ocean and Cryosphere in a Changing Climate* (eds Portner, H.-O. et al.) 3–35 (Cambridge University Press, Cambridge, UK and New York, NY, USA, 2019).

30. Boral, S. et al. Tracking dissolved trace and heavy metals in the Ganga River from source to sink: a baseline to judge future changes. *Geochem. Geophys. Geosyst.* **21**, 009203 (2020).
31. Bhatia, M. et al. Greenland meltwater as a significant and potentially bioavailable source of iron to the ocean. *Nat. Geosci.* **6**, 274–278 (2013).
32. Tipper, E. T. et al. The short term climatic sensitivity of carbonate and silicate weathering fluxes: Insight from seasonal variations in river chemistry. *Geochim. Cosmochim. Acta* **70**, 2737–2754 (2006).
33. Colombo, N. et al. Influence of permafrost, rock and ice glaciers on chemistry of high-elevation ponds (NW Italian Alps). *Sci. Total Environ.* **685**, 886–901 (2019).
34. Hopwood, M. J. et al. Highly variable iron content modulates iceberg-ocean fertilisation and potential carbon export. *Nat. Commun.* **10**, 5261 (2019).
35. Lencioni, V. et al. Metal enrichment in ice-melt water and uptake by chironomids as possible legacy of World War One in the Italian Alps. *Chemosphere* **340**, 139757 (2023).
36. Hodson, A. J., Mumford, P. N., Kohler, J. & Wynn, P. M. The High Arctic glacial ecosystem: new insights from nutrient budgets. *Biogeochemistry* **72**, 233–256 (2005).
37. Fell, S. C. et al. The multitrophic effects of climate change and glacier retreat in mountain rivers. *Bioscience* **67**, 897–911 (2017).
38. Lohan, M. C., Statham, P. J. & Moore, C. M. Importance of trace elements micronutrients for marine microorganisms. In *Marine Bioinorganic Chemistry* (ed. Hunter, K. A.) 113–143 (Springer, 2015).
39. Gaillardet, J., Viers, J. & Dupré, B. Trace elements in river waters. In *Treatise on Geochemistry* Vol. 7 (eds Holland, H. D. & Turekian, K. K.) 195–235 (Elsevier, 2014).
40. Al-Momani, I. F. Trace elements in atmospheric precipitation at northern Jordan measured by ICP-MS: acidity and possible sources. *Atmos. Environ.* **37**, 4507–4515 (2003).
41. Bruland, K. W., Middag, R. & Lohan, M. C. Controls of trace elements in seawater. In *Treatise on Geochemistry* 2nd edn (eds Holland, H. D. & Turekian, K. K.) 19–51 (Elsevier, 2014).
42. Dong, Z. et al. New insights into trace elements deposition in the snow packs at remote alpine glaciers in the northern Tibetan Plateau, China. *Sci. Total Environ.* **529**, 101–113 (2015).
43. Raiswell, R. Trace metals in carbonates—a brief review. *Mar. Geol.* **62**, 153–166 (1984).
44. Wedepohl, K. H. The composition of the continental crust. *Geochim. Cosmochim. Acta* **59**, 1217–1232 (1995).

Acknowledgements

We gratefully acknowledge the Wadia Institute of Himalayan Geology (Dehradun) and the National Institute of Hydrology (Roorkee) for providing field and laboratory facilities. S.S. acknowledges support from the Department of Science and Technology, Government of India (Women Scientist Scheme, SR/WOS-A/EA-44/2016), and the Gansu Postdoctoral Science Foundation (E439880109). T.S. acknowledges support from the Talent Program Category B of the Northwest Institute of Eco-Environment and Resources, CAS (E329010501), Ministry of Human Resources and Social Security, Gansu, China (E490010101). We are grateful to the editor and all three reviewers for their insightful and constructive feedback, which significantly enhanced the clarity, structure, and overall quality of the paper.

Author contributions

S.S., T.S., and S.K. designed research; S.S., T.S., and D.P.D. performed research; S.S., T.S., and R.S. analyzed data; S.K., Y.Z., U.B., R.S., and D.P.D. provided review and suggestions; and S.S., T.S. prepared figures and T.S. wrote the article with contributions from all other co-authors.

Competing interests

The authors declare no competing interests.

Additional information

Supplementary information The online version contains supplementary material available at https://doi.org/10.1038/s43247-025-03064-9.

Correspondence and requests for materials should be addressed to Tanuj Shukla.

Peer review information *Communications Earth and Environment* thanks Stefano Brighenti and the other, anonymous, reviewer(s) for their contribution to the peer review of this work. Primary Handling Editors: Sadia Ilyas and Somaparna Ghosh [A peer review file is available].

Reprints and permissions information is available at http://www.nature.com/reprints

Publisher's note Springer Nature remains neutral with regard to jurisdictional claims in published maps and institutional affiliations.

Open Access This article is licensed under a Creative Commons Attribution-NonCommercial-NoDerivatives 4.0 International License, which permits any non-commercial use, sharing, distribution and reproduction in any medium or format, as long as you give appropriate credit to the original author(s) and the source, provide a link to the Creative Commons licence, and indicate if you modified the licensed material. You do not have permission under this licence to share adapted material derived from this article or parts of it. The images or other third party material in this article are included in the article's Creative Commons licence, unless indicated otherwise in a credit line to the material. If material is not included in the article's Creative Commons licence and your intended use is not permitted by statutory regulation or exceeds the permitted use, you will need to obtain permission directly from the copyright holder. To view a copy of this licence, visit http://creativecommons.org/licenses/by-nc-nd/4.0/.

© The Author(s) 2026